PARTIALLY FILLED AKR EMISSION CONES

R. Schreiber*

Abstract

Two dynamic spectra collected with Polrad swept frequency analyzer onboard Interball-2 mission are used to illustrate AKR beaming. Beams are discussed in terms of AKR directivity pattern mapping on the single dynamic spectrum. Long-lived bright lanes in the spectra are explained as a consequence of satellite path intersection with the conical sheets within AKR emission cone. For two cases shown in this paper its angular thickness can vary between tens of degrees and about 1°.

1 Introduction

The question of emission directivity emerged in the early years of AKR observations. Based mostly on statistical reasoning, the geometrical concept of AKR emission cone (as a region in space filled more or less uniformly with radiation) was introduced [Green et al., 1977; Green and Gallagher, 1985]. Alternatively, the possibility of emission cone filling (or hollowness) was discussed by Calvert [1981, 1987] and Zarka [1988]. This short paper presents an example of reexamination in terms of structure of the AKR emission cone of such dynamic spectra morphological features as the shape of lower frequency cutoff, long-lasting structures in the dynamic spectra, or AKR beams. Presented cases are drawn from Polrad experiment data taken onboard Interball-2 mission [Hanasz et al., 1998] for the observations of Earth's northern hemisphere.

2 Model

A very simple model of AKR propagation and directivity used in this paper is centered on the concept of the emission cone. No ray tracing has been applied, which means rectilinear propagation along the whole raypath. For the cases presented, the raypaths were not influenced by the presence of the plasmasphere.

* *Space Research Centre PAS, Warsaw, Poland*

2.1 Emission cone

In this paper, a cylindrically symmetric thin conical sheet with its axis tangent to the direction of the magnetic field in the source represents the elementary AKR emission diagram. It is parameterized by its half-opening angle. Choosing different angles, it is possible to define smaller (embedded) sheets. A set of angles delimited by the external and internal opening angles defines a partially filled cone or beam (if AKR is emitted only within a part of the perimeter). A filled emission cone can be represented by a set of opening angles filling the whole range between 0° and the biggest opening angle. A set of cones distributed along the magnetic field line passing through the AKR source represents AKR emitted at different frequencies. A given AKR frequency corresponds to the local electron gyrofrequency at the source. The assumption of AKR emission pattern cylindrically symmetric with respect to the magnetic field direction at the source generally does not hold for the R-X mode prevailing in AKR and strongly refracted close to the source [Calvert, 1987]. But for the purpose of this paper it has been retained - from full 3D ray tracing for the realistic case of VIKING AKR observations [de Feraudy and Schreiber, 1995] it can be concluded that for their particular case the cone symmetry axis is tilted about 5° to the North with respect to the magnetic field direction at the source. On the other hand, for cases shown in this paper only part of the emission cone perimeter is crossed during the dynamic spectra recording. The third reason for keeping such simple approximation consists in the illustrative purpose of the paper - its basic aim is to demonstrate the possibility of identifying some morphological features in the dynamic spectrum with the AKR radiation pattern.

Two assumptions are important for the model:

- small source region sizes delimited by a relatively narrow bunch of magnetic field lines — ±2° in Invariant Latitude and ±0.5 h in MLT (or about 500 × 500 km at the magnetic field line footprint for 70° Invariant Latitude) — in such a situation a segment of a single magnetic field line can represent the AKR source in our model).
- the source position stable within tens of minutes.

Such conditions cannot be granted for all our AKR observations. The choice of relevant dynamic spectra was based mainly on the presence of smooth, bowl-shaped lower frequency cut-off and bright lanes within the dynamic spectrum parallel to this cut-off. The possibility of obtaining a satisfactory fit of the model to the data was an a posteriori evidence of validity of these assumptions for a particular AKR case analyzed. Other dynamic spectra produced, for instance, by multiple sources or by irregular emissions will not fit the simple scenario used in this paper. Not much is known about AKR sources spacing — Louarn and Le Quéau [1996] report the crossing of a double AKR source, Schreiber et al. [2002] discuss switching of AKR activity between two sources within a 30–minute period and Mutel et al. [2003] determine statistical sizes of AKR sources projected on the auroral oval for six different epochs for periods of 1–3 hours - they vary between 1000 and 4000 km. Unfortunately, there is no discussion of the overall source intensity distribution changes in time, Mutel et al. measure positions of very short AKR bursts (a single data

window lasts about 300 ms). Possible radiation scattering close to the source region can also account for the apparently big sizes of the AKR sources.

2.2 Mapping of AKR beams onto dynamic spectra

During AKR visibility period, the spacecraft moving along its orbit crosses successive parts of the AKR emission cone. The lower frequency cutoff of the AKR dynamic spectrum corresponds to the moments of entering emission cone for different frequencies emitted at the source region. Structures above that line correspond to the elements of AKR radiation pattern contained inside of the emission cone. For every point of the dynamic spectrum (also for those outside of the AKR emissions) we determine two angles - they describe the geometrical position of the spacecraft with respect to the source region and do not necessarily correspond to the filled parts of the AKR radiation pattern:

- emission angle between the direction from the source to the observer and the direction antiparallel to the local magnetic field direction at the source (sources in question are located on the northern hemisphere) - its greatest value corresponds to the emission cone half-opening angle. The next step consists in producing a contour plot labelled by constant emission angles and in superposing it onto the dynamic spectrum (solid lines in Fig.1 and Fig.2). These angles are chosen starting from 90° and successive curves are plotted for values decremented by 10° (or 5° if necessary).
- azimuthal angle of the direction from the source to the observer measured in the plane perpendicular to the local magnetic field line at the source - starting from West (0°) through South (90°) to East (180°). A contour plot containing constant azimuth angle curves has been also superposed on the dynamic spectrum (dotted lines). For some azimuths AKR will reach the observer, for other not — it can be a result of leaving the emission cone or of AKR beaming.

If within the emission cone there exist conical sheets delimiting regions of enhanced emissions, such regions will map onto the dynamic spectrum as bright lanes parallel to the closest constant emission angles curves. The constant emission angle - azimuth grid superposed onto the dynamic spectrum can help to isolate specific morphological features. As it will be shown later, such a seemingly artificial concept can work fairly well for the real data. Detailed discussion of the model can be found in Schreiber, [2005].

3 Observations

Two data examples are shown in Fig.1 and Fig.2. Both were collected by Polrad experiment onboard Interball-2 probe [Hanasz et al., 1998]. Orbital parameters of the satellite launched on August 29, 1996 were: inclination 62.8°, apogee 19140 km above Earth's surface, and perigee at 772 km. Dynamic spectra were recorded by the Polrad step frequency analyzer swept over 4 kHz – 0.5 MHz frequency range, with repetition period of 6 s and a frequency resolution of 4 kHz. In one of its working modes Polrad was working as a polarimeter registering all 4 Stokes parameters of the AKR radiation.

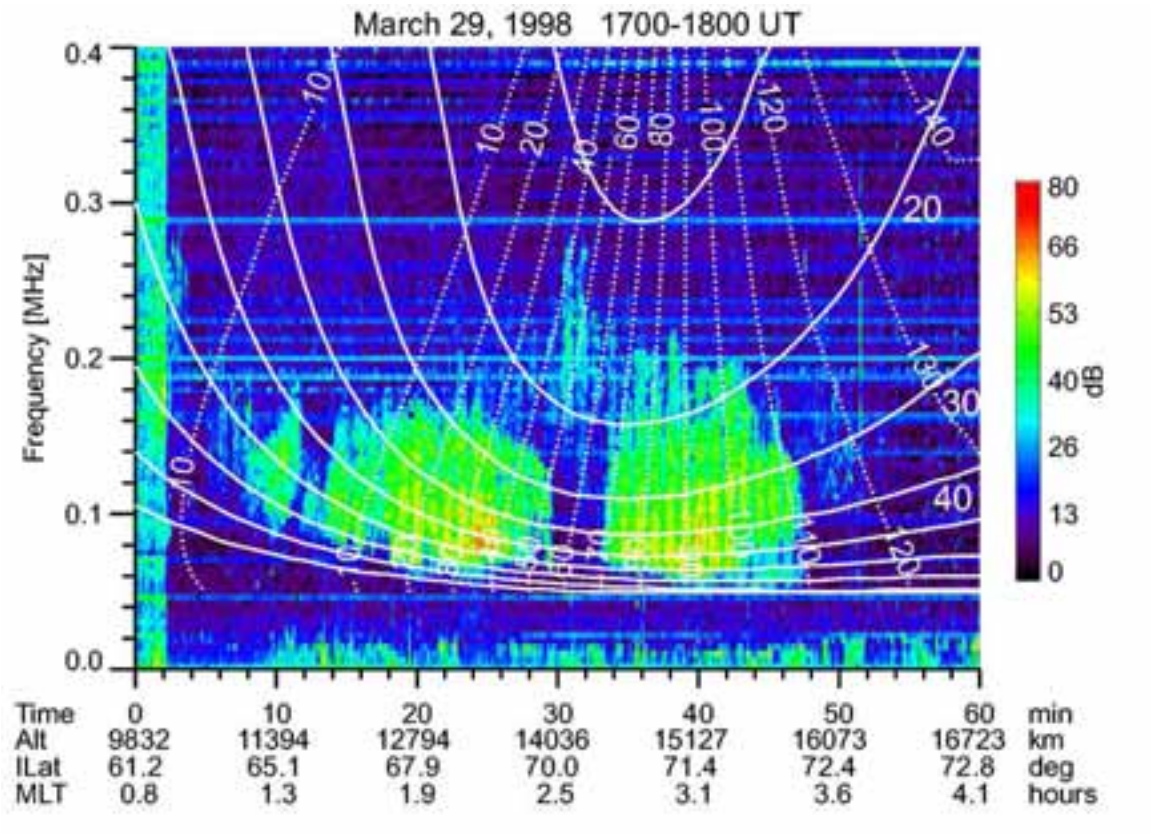

Figure 1: Example of a partially filled AKR emission cone about 40°–50° thick (left part of the dynamic spectrum). The right part probably corresponds to another, much wider beam. White arrows show the approximate latitudinal extent of the emission cone. White solid lines separated by 10° correspond to the given emission cone half-opening angle. Dotted lines represent azimuthal angle measured in the plane perpendicular to the magnetic field direction in the source (also separated by 10°)

4 Application of the model

Two figures illustrate the basic idea of the paper. Fig.1 represents an AKR with most probably partially filled emission cone — till 1725 UT the upper boundary of the dynamic

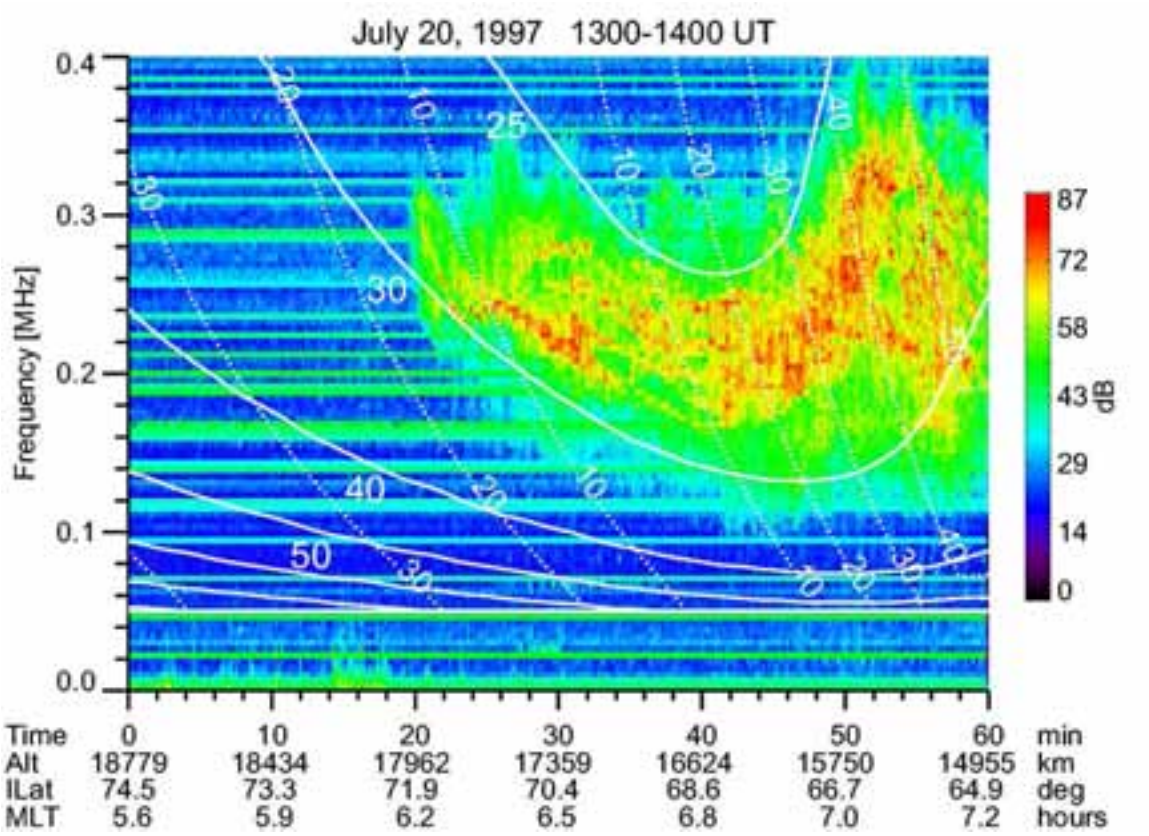

Figure 2: Dynamic spectrum corresponding to a partially filled emission cone with small half-opening angle (about 30°) and a rather thin wall (less than 10°). White arrows show the approximate latitudinal extent of the cone, the black ones follow very narrow angular structures in the spectrum.

spectrum corresponds to $f \simeq$ const., probably referring to the lower physical boundary of the AKR source region. For the next 5 minutes, the upper boundary is parallel to the line of the constant emission angle pointing towards crossing of the partially filled emission cone. The situation is changing with time and the cone corresponding to the right part of the dynamic spectrum seems to be more filled (and less stable) than on the left side. Azimuth for both AKR bursts spans more than 100°. Between 17:30 UT and 17:32 UT there is 20° an interesting (unexplained at the present moment) azimuthal gap filled partially with much weaker AKR radiation. The second figure shows a narrow emission cone with embedded very thin sheets. The AKR emission is confined to a conical sheet about 5° thick, the thin structures are likely less than 1° wide. They resemble structures (arcs) recently reported for Jupiter's DAM emissions by Kaiser et al., [2000]. Azimuth spans here about 70°.

5 Discussion

The simple model applied in this paper works well when the position of the AKR source is known. For most of Polrad's dynamic spectra we do not have that sort of data. Direction

finding method for our data based on polarization measurements [Panchenko, 2004] has been applied until now only to a small number of dynamic spectra. Nevertheless, fitting of the constant emission angle curves to the AKR dynamic spectra (especially to its lower frequency cut-off and at the same time to bright lanes present in the dynamic spectrum) offers a fairly good solution of the problem. The AKR source size limit $\pm 2^\circ$ in Invariant Latitude and ± 0.5 h in MLT was derived from the fitting procedure - details can be found in a paper by Schreiber, [2005]. Only part of our data ($\approx 20\%$) can be analyzed in the way discussed in this paper. Many AKR realizations consist of a suite of successive bursts probably produced by different source regions. The geometrical factor plays an important role - nice fits can be expected for spacecraft passing relatively close to the source region where changes in the lower frequency cut-off are much quicker than for spacecraft on the orbit tangent to the auroral oval. Another, more acute problem consists in deciding whether the restricted azimuth range for some structures (like two parts of the dynamic spectrum in Fig.1) has anything to do with restricted sizes of the AKR beams, or corresponds to the emission duration in time. This probably cannot be answered while using single spacecraft observations.

6 Conclusions

The simple assumption of the stability of AKR source position and its emission angular pattern during tens of minutes is sufficient to explain the shape of low frequency cut-off as well as the existence of bright lanes within some of the AKR dynamic spectra. These lanes, parallel to the spectrum lower frequency cut-off, can be treated as a result of the spacecraft crossing the conical sheets embedded into AKR emission cone. For two cases shown in this paper, its angular thickness can vary between tens of degrees and about 1°.

Acknowledgments

I am grateful to Joelle Durand and her team (CNES Toulouse) for preprocessing the Polrad data. This work was partially supported by the Committee of the Scientific Research in Poland, grant no. 5 T12E 001 22.

References

Calvert, W., The signature of Auroral kilometric radiation on ISIS 1 Ionograms, *J. Geophys. Res.*, **86**, 76, 1981.

Calvert, W., Hollowness of the observed auroral kilometric radiation pattern, *J. Geophys. Res.*, **92**, 1267, 1987.

de Feraudy, H. and R. Schreiber, Auroral radiation ray distribution in the light of Viking observations of AKR, *Geophys. Res. Lett.*, **22**, 2973, 1995.

Green, J. L., D. A. Gurnett, and S. D. Shawhan, The angular distribution of auroral kilometric radiation, *J. Geophys. Res.*, **82**, 1825, 1977.

Green, J. L., and D. L. Gallagher, The detailed intensity distribution of the AKR emission cone, *J. Geophys. Res.*, **90**, 9641, 1985.

Hanasz, J., R. Schreiber, H. de Feraudy, M. M. Mogilevsky, and T. V. Romantsova, Observations of the upper frequency cutoffs of the Auroral Kilometric Radiation, *Annales Geophysicae*, **16**, 1097, 1998.

Kaiser, M. L., P. Zarka, W. S. Kurth, G. B. Hospodarsky, and D. A. Gurnett, Cassini and Wind stereoscopic observations of Jovian nonthermal radio emissions: Measurement of beam widths, *J. Geophys. Res.*, **105**, 16053, 2000.

Louarn, P., and D. Le Quéau, Generation of the Auroral Kilometric Radiation in plasma cavities: - I. Experimental study, *Planet. Space Sci.,* **44,** 199, 1996.

Mutel, R. L., D. A. Gurnett, I. W. Christopher, J. S. Pickett, and M. Schlax, Locations of auroral kilometric radiation bursts inferred from multispacecraft wideband Cluster VLBI observations. 1: Description of technique and initial results, *J. Geophys. Res.*, **108**(A11), 1398, doi:10.1029/2003JA010011, 2003.

Panchenko, M., Direction finding of AKR sources with three orthogonal antennas, *Radio Sci.*, **38(6)**, 1099, doi:10.1029/2003RS002929, 2003.

Schreiber, R., O. Santolik, M. Parrot, F. Lefeuvre, J. Hanasz, M. Brittnacher, and G. Parks, Auroral kilometric radiation source characteristics using ray tracing techniques, *J. Geophys. Res. (Space Physics)*, A11, 20–1, 2002.

Schreiber, R., A simple model of the auroral kilometric radiation visibility, *J. Geophys. Res.*, **110**, A11222, doi:10.1029/2004JA010903, 2005.

Zarka, P., Beaming of planetary radioemissions, in *Planetary Radio Emissions II*, H. O. Rucker, S. J. Bauer, and B. M. Pedersen (eds.), Austrian Academy of Sciences Press, Vienna, 327, 1988.